Gravitational-wave detectors cooled with superfluid helium – GRAVITHELIUM

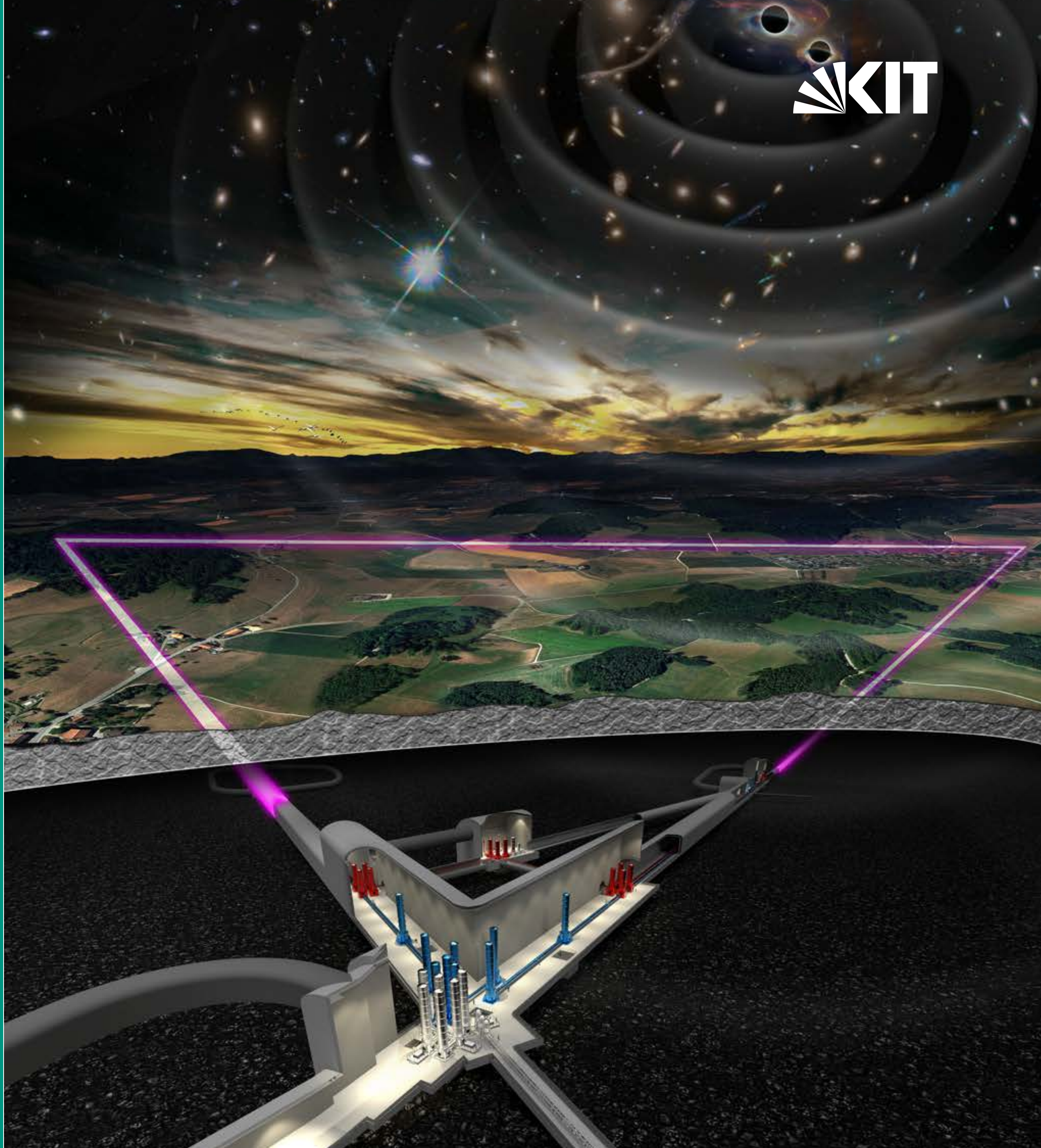

Steffen Grohmann, Xhesika Koroveshi, Enes Turkic and Timo Weckerle, Karlsruhe Institute of Technology

LT30, August 7-13, 2025, Bilbao, Spain

Outline

1. Gravitational-wave detection by laser interferometry
2. He-II cooling concept for cryogenic mirrors
3. ERC project GRAVITHELIUM

Gravitational-wave (GW) detection by laser interferometry

01

Brief history of gravitational-wave detection

1916 **Postulation** of gravitational waves by Albert Einstein

2015 **First** direct GW **detection**

2017 **Synchronous detection** at LIGO (US) and VIRGO (Pisa, IT)

GW150915 PRL 116, 061102 (2016)

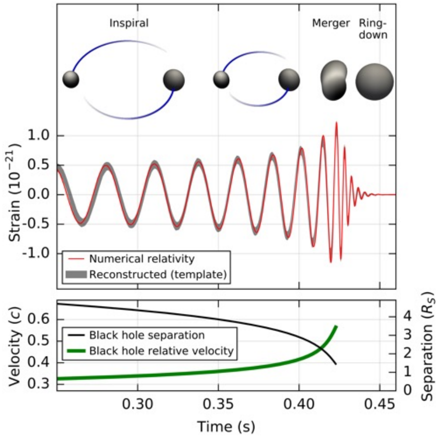

Source: B. P. Abbott et al. Phys. Rev. Lett. 116, 061102, doi 10.1103/PhysRevLett.116.061102

GW170817 + GRB170817A + AT 2017gfo

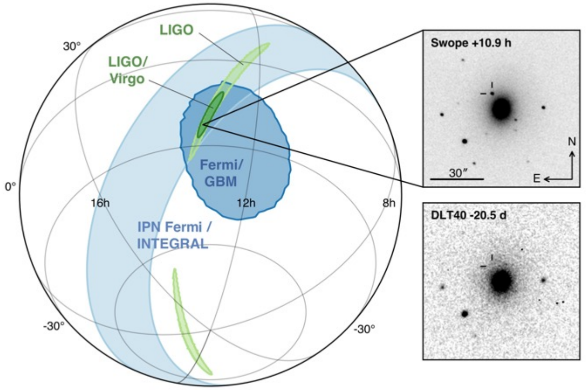

Source: B. P. Abbott et al 2017 ApJL 848 L12, doi: 10.3847/2041-8213/aa91c9

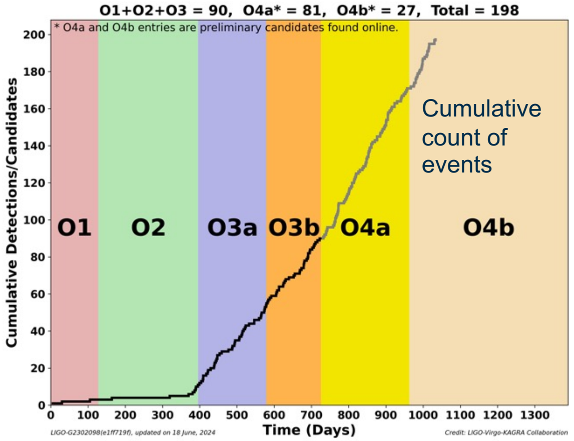

Source: https://dcc.ligo.org/LIGO-G2302098-v15/public

2017 **Nobel prize in physics** for R. Weiss, B. Barish, K. Thorne (**GW detection**)

2020 **Nobel prize in physics** for R. Penrose, R. Genzel, A. Ghez (**Black holes**)

GW detection principle

Check

Michelson interferometer

- Laser through beam splitter
- Reflection at end mirrors (test masses)
- Extinction at identical arm lengths
- Signal due to GW length deformation
- Sensitivity needed: $\Delta L \approx \mathbf{10^{-19}\ m}$

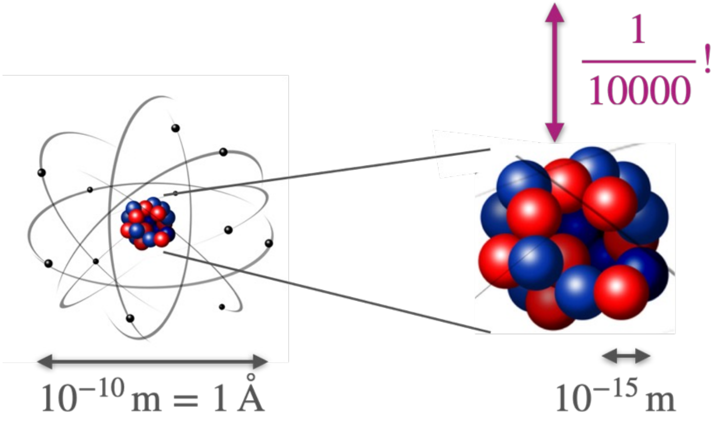

LIGO layout

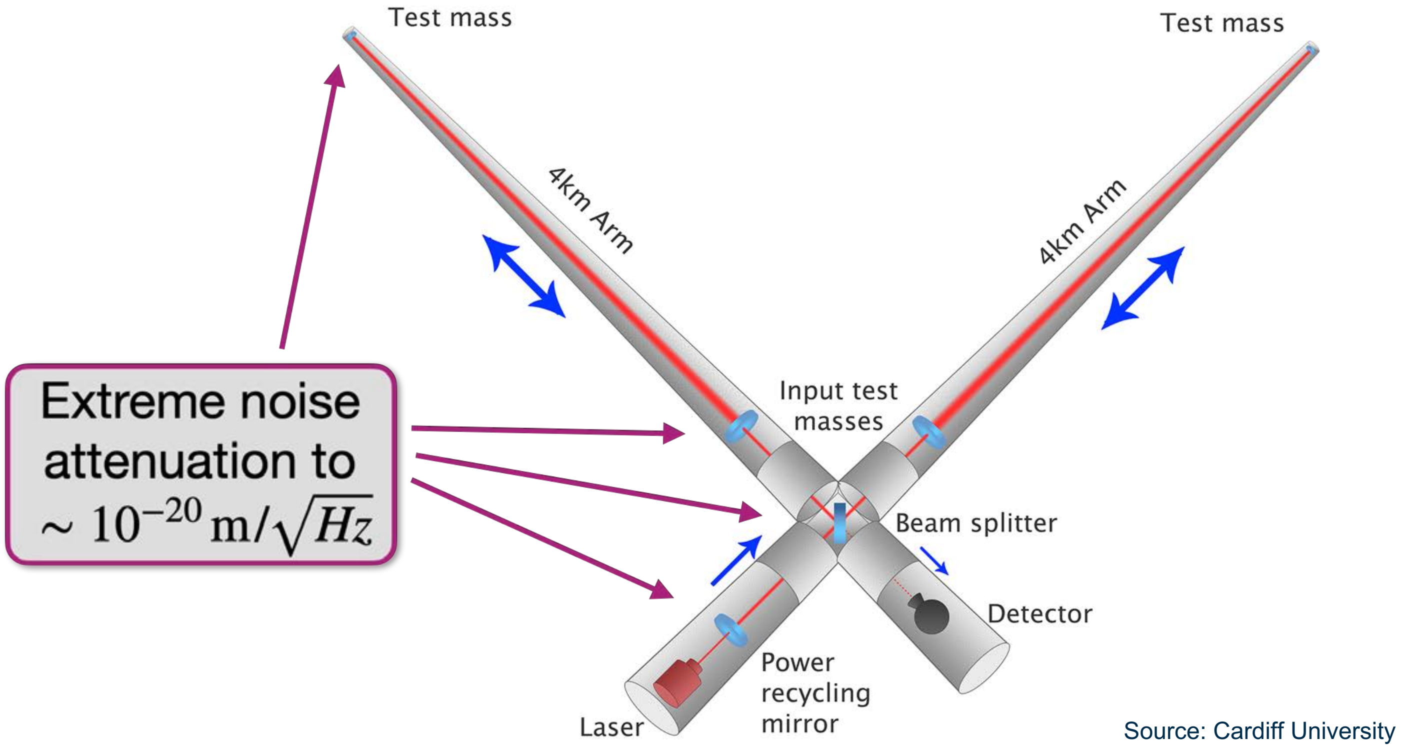

Source: Cardiff University

ET detection horizon for black hole binaries

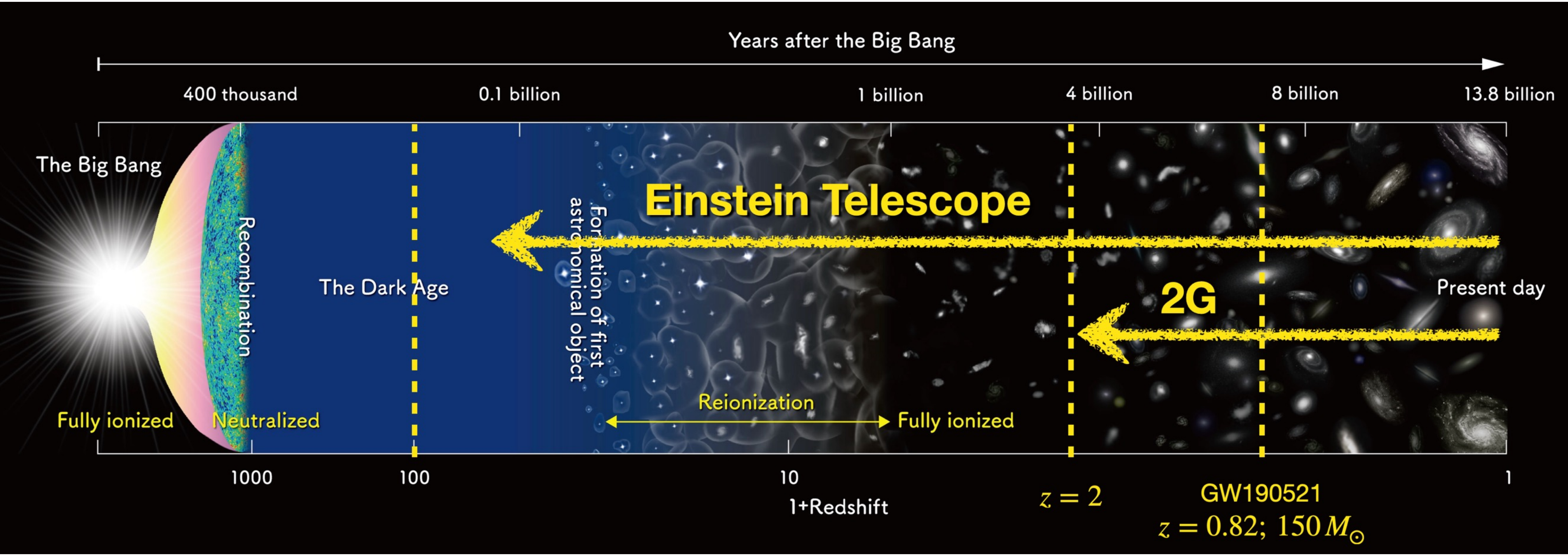

Credit: ALMA Collaboration

Challenge of ET: Create the QUIETEST place on earth

LIGO / Virgo (2G)

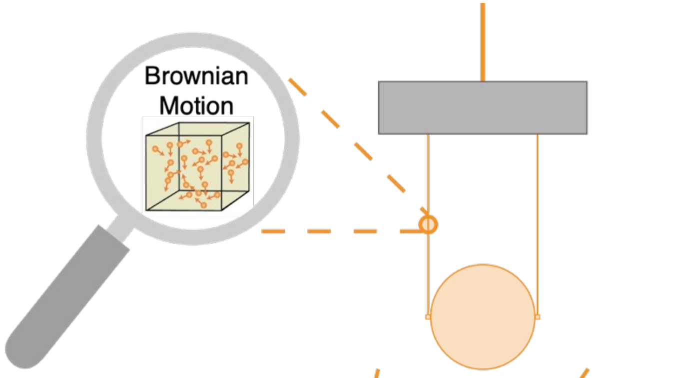

ET (3G)

Cryogenic operation is a **new key technology** to limit the suspension thermal noise (STN) at low frequency (ET-LF)

- $T_{\mathrm{Mirror}} = 10 \ldots 20\ \mathrm{K}$

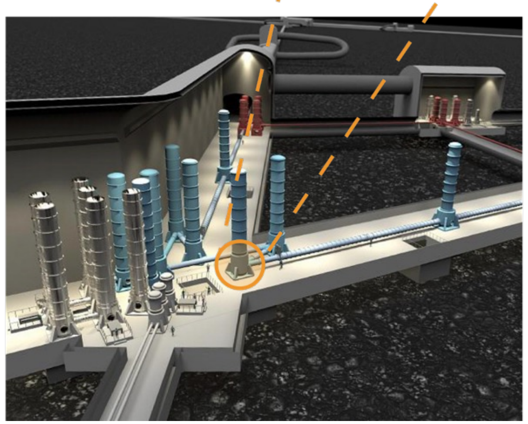

Limiting fundamental noises at low frequency

Source: M. Branchesi et al.: Science with the Einstein Telescope: A comparison of different designs. arXiv:2303.15923 [gr-qc] (2023)

Comparison of low-frequency sensitivities

- Adv. Virgo / Adv. LIGO (2G): $f_{\mathrm{min}} = 10\ \mathrm{Hz}$
- KAGRA (2.5G): $f_{\mathrm{min}} = 5\ \mathrm{Hz}$
- ET (3G): $\boldsymbol{f_{\mathrm{min}} = (2)3\ \mathrm{Hz}}$ (5 Hz sensitivity $\times\, 10^{-3}$)

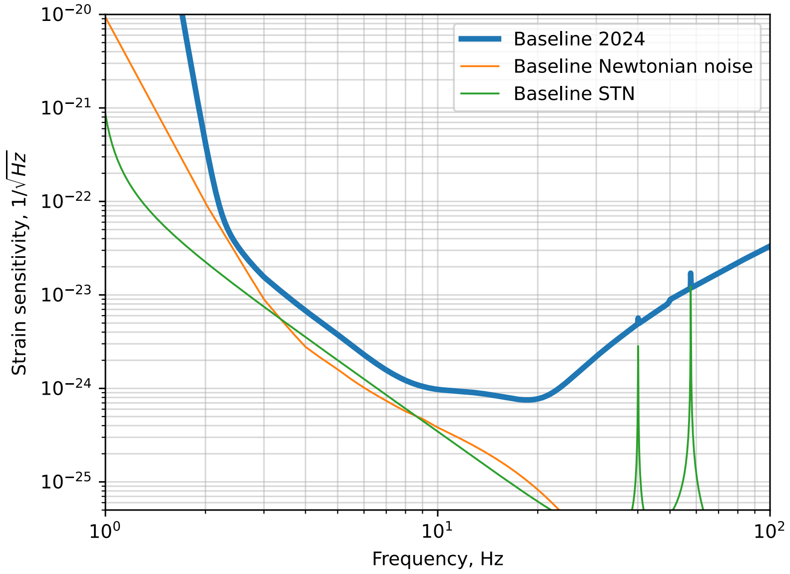

Credit: Mikhail Korobko, ET-Noise Budget Gitlab - PyGwinc Code (29.05.2025)
https://gitlab.et-gw.eu/et/isb/interferometer/ET-NoiseBudget

The low-frequency sensitivity is crucial for exploiting the full scientific potential of ET, in particular with regard to:

- the observation of binary neutron stars (BNS), staying long time in the bandwidth,
- pre-merger detection to probe the central engine of gamma ray bursts (GRB), particularly to understand the jet composition, the particle acceleration mechanism, the radiation and energy dissipation mechanisms,
- detecting a large number of kilonovae counterparts,
- detecting primordial black holes (PBH) at redshifts $z > 30$, and
- detecting intermediate massive back holes (IMBH) in the range of $10^2 - 10^4\ M_\odot$.

Detector layout of the Einstein Telescope

Separation of detection frequency band

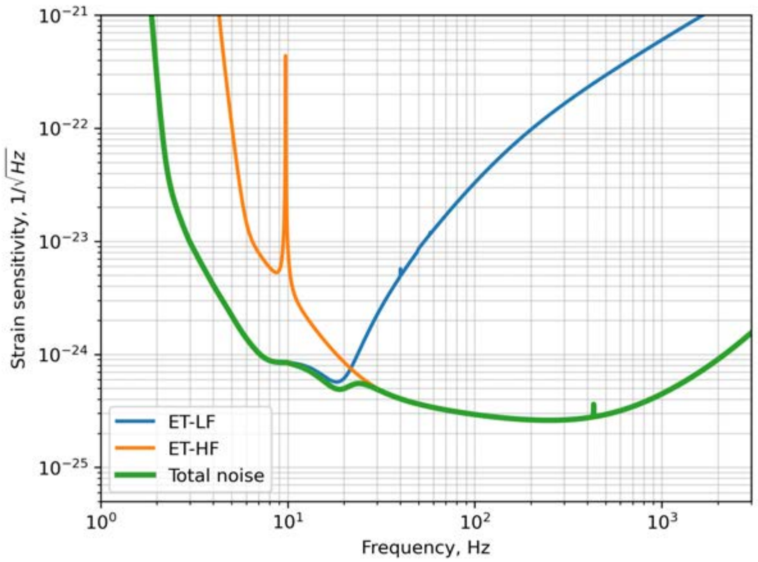

Credit: Mikhail Korobko, ET-Noise Budget Gitlab - PyGwinc Code (4.8.2025) https://gitlab.et-gw.eu/et/isb/interferometer/ET-NoiseBudget

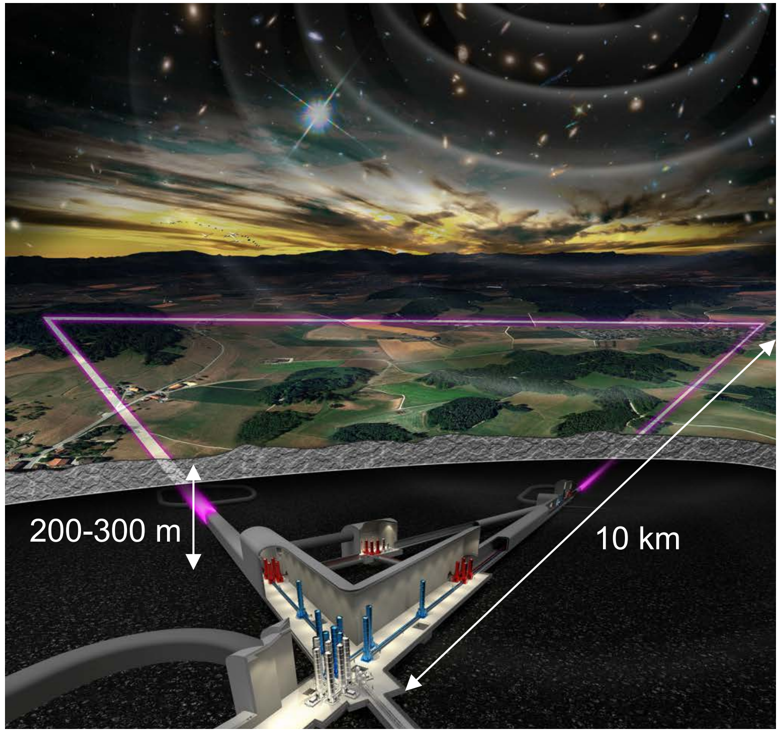

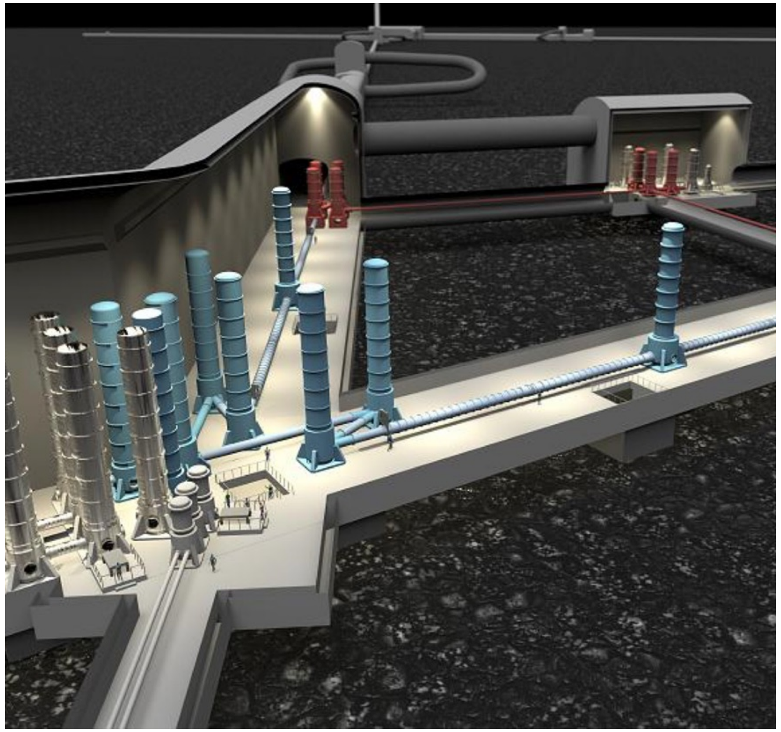

- **ET-LF:** (2)3…30 Hz, 18 kW laser power, cryogenic optics 10…20 K
- **ET-HF:** 30 Hz …10 kHz, 3 MW laser power, room-temperature optics

- Original 10 km triangular single-site configuration
- Alternative 15 km double-L two-site configuration under investigation

- Underground installation of large vacuum towers and beam pipes
- Four cryogenic towers in each vertex

ET-LF test mass tower and cryostat configuration

Tower layout

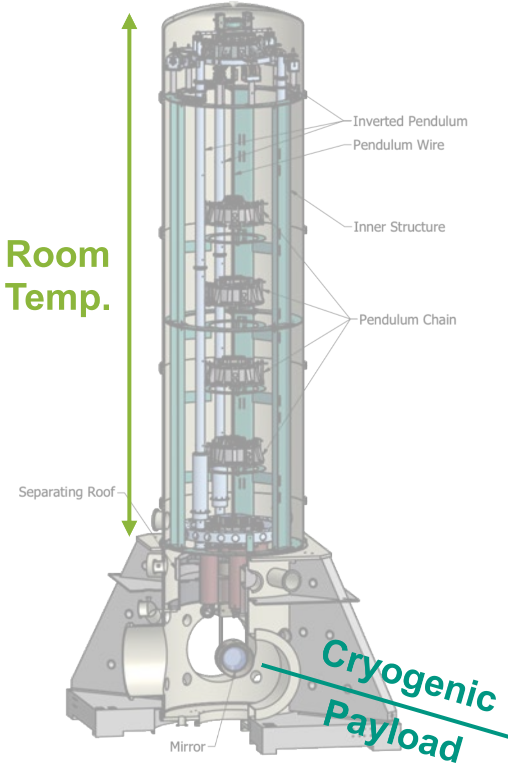

Source: ET Design Report Update (2020)

KAGRA mirror (23 kg)
https://www.nao.ac.jp/

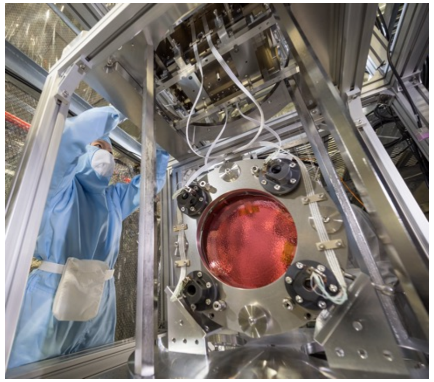

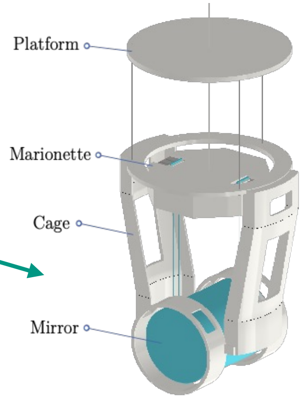

ET-LF payload

$h \approx 3.5$ m

$m_{\text{total}} \leq 1000$ kg

$m_{\text{Mirror}} \approx 200$ kg

Conceptual cryostat layout

- Challenge: **Human access** inside cryostats assuring cleanroom conditions!

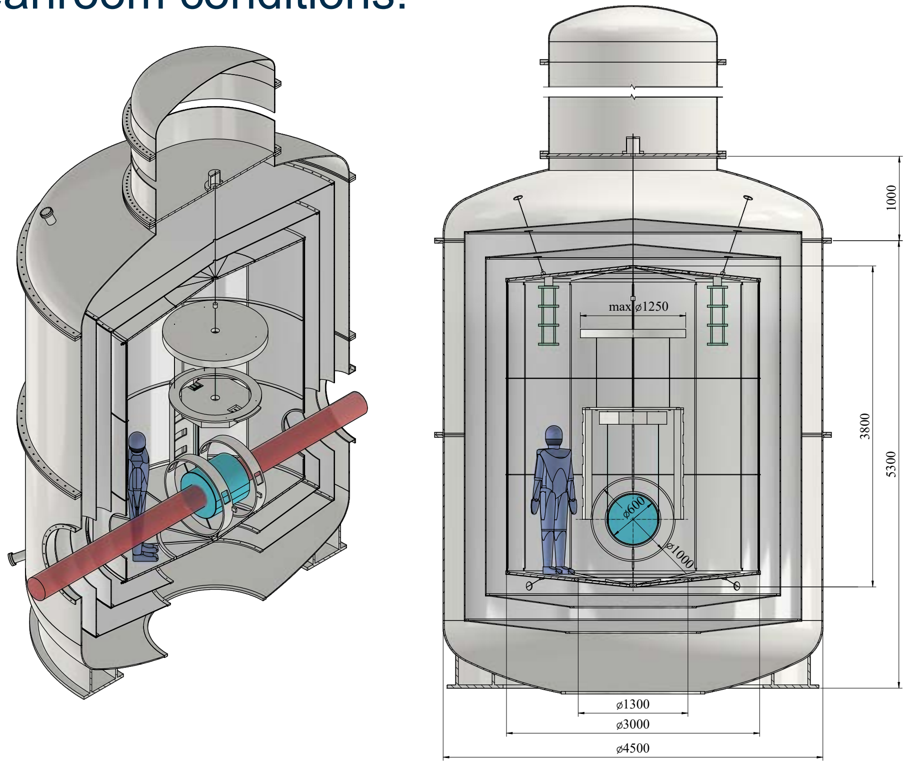

He-II cooling concept for cryogenic mirrors

02

Payload cooling with superfluid helium (He-II)

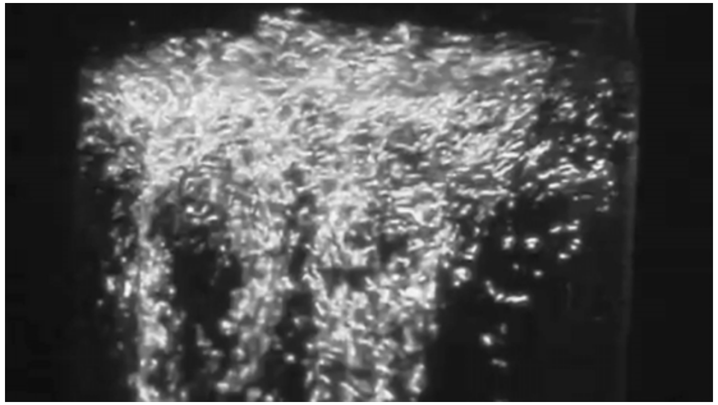

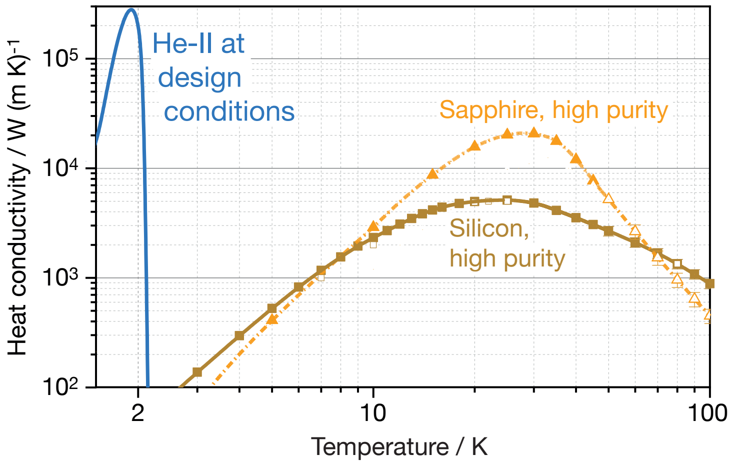

He-II:
The quietest medium to absorb heat

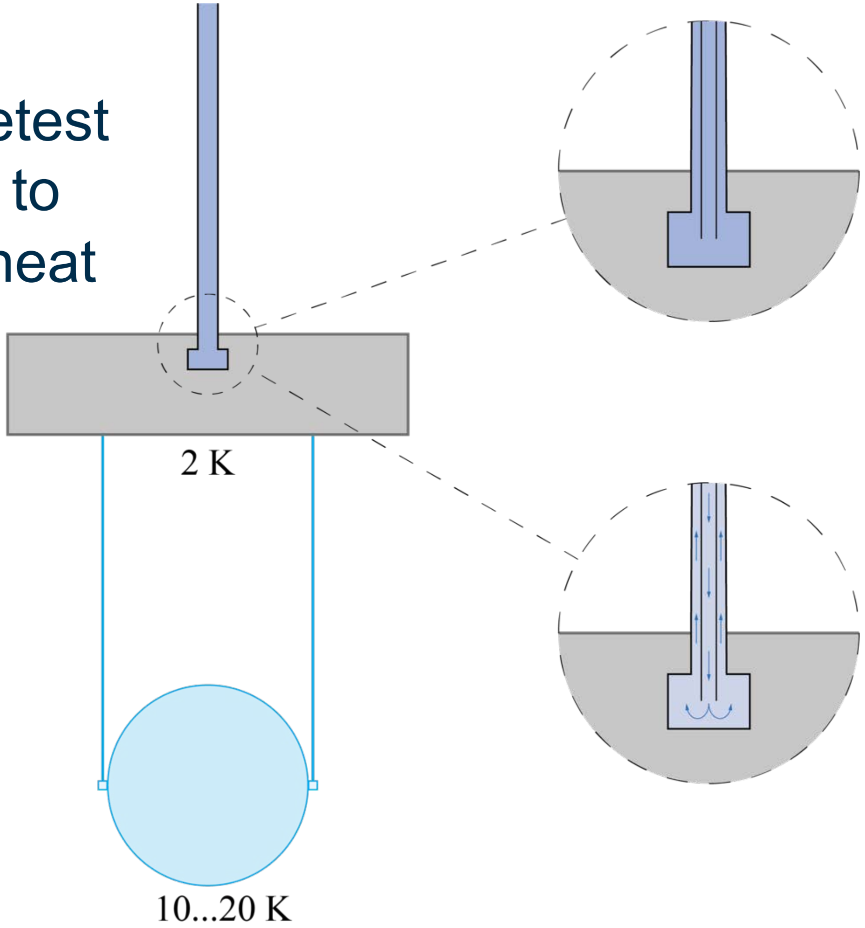

Steady-state:
Static He-II

Cool-down:
He-I counter-flow

Theoretical proof of He-II concept

Baseline design of ET-LF payload

- First consistent **thermal**, **mechanical** and **STN** modeling
- Study of two cooling options

Reference: Koroveshi X, Busch L, Majorana E, Puppo P, Rapagnani P, Ricci F, Ruggi P, Grohmann S, Phys.Rev. D (2023), DOI: 10.1103/PhysRevD.108.123009

Conventional concept

- Monocrystalline rod
- 6N Al heat links attached to cage and platform

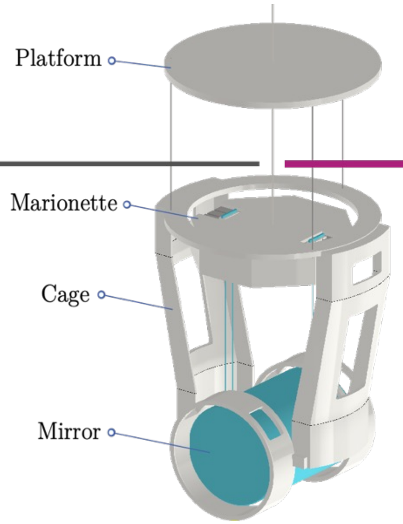

He-II concept

Titanium tube filled with static He-II

Results of STN modeling

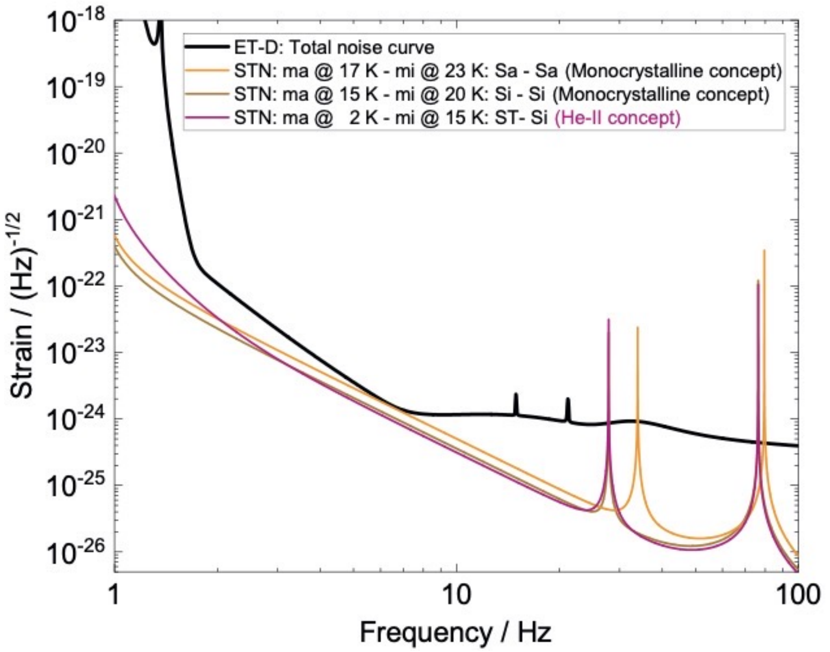

- 2 K Ti tube is feasible, but how does the He-II contribute to the STN?
- ➢ **Experimental investigation** needed

Funded by the European Union
European Research Council
Established by the European Commission

GRAVITHELIUM

Gravitational Wave Detectors Cooled with Superfluid Helium

ERC project GRAVITHELIUM

03

OBJECTIVES of GRAVITHELIUM

Phase 2: He-II suspensions

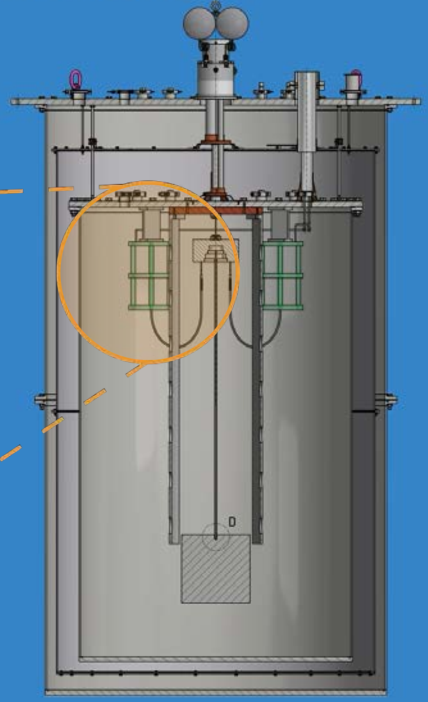

KEY TECHNOLOGY development

Lab-scale He-II supply and vibration attenuation system

Cooperation with industry partner

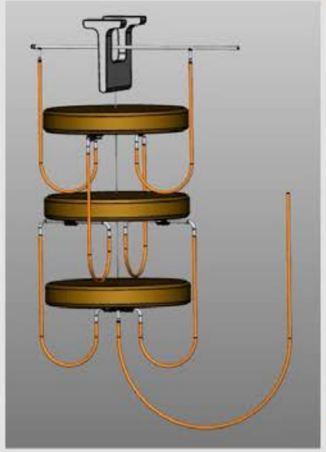

Phase 1:

Solid state suspensions

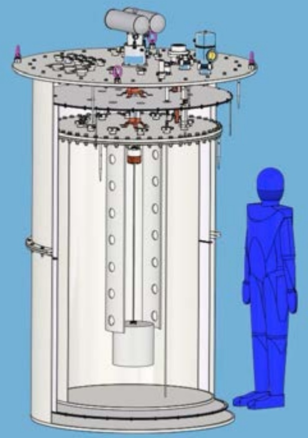

Physical data on dissipation in cryogenic payload suspensions

Experimental method

- Investigation of dissipation mechanisms by Q-factor measurements
  - $Q^{-1} = \phi(\omega_0)$, i.e., loss angle at resonance
  - $\phi_{\text{susp}} = \phi_{\text{bulk}} + \phi_{\text{thermoelastic}} + \phi_{\text{surface}} + \phi_{\text{extrinsic}}$

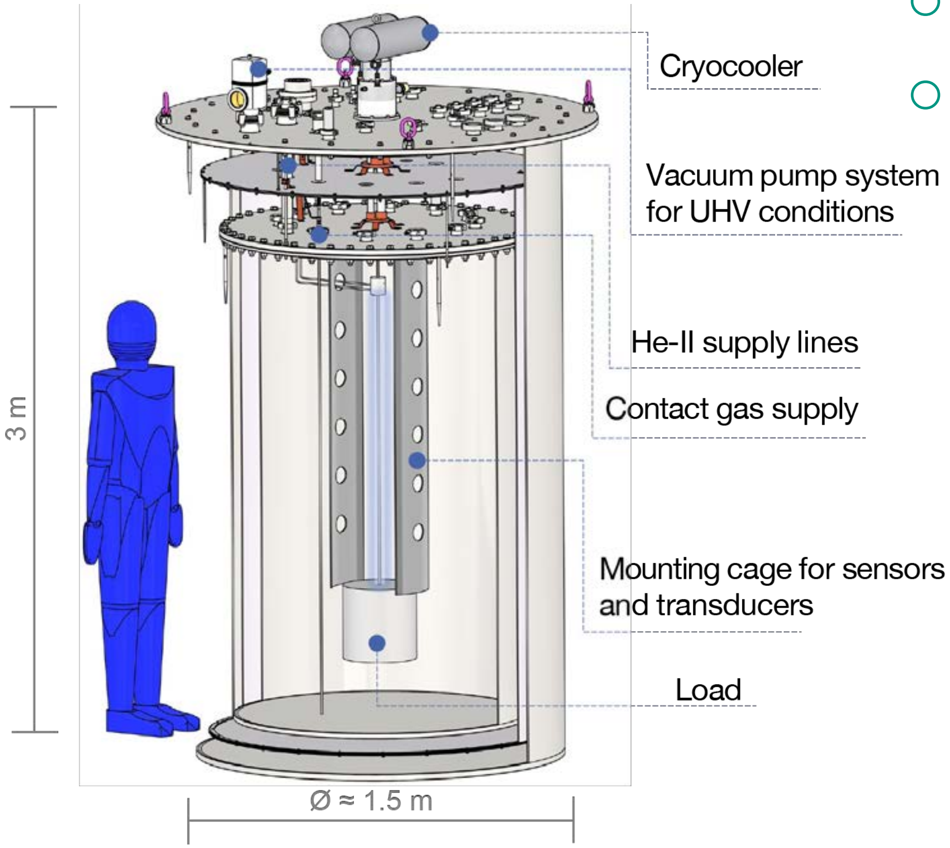

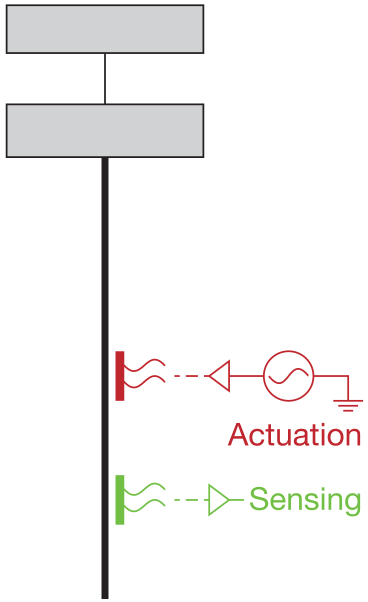

Intrinsic losses

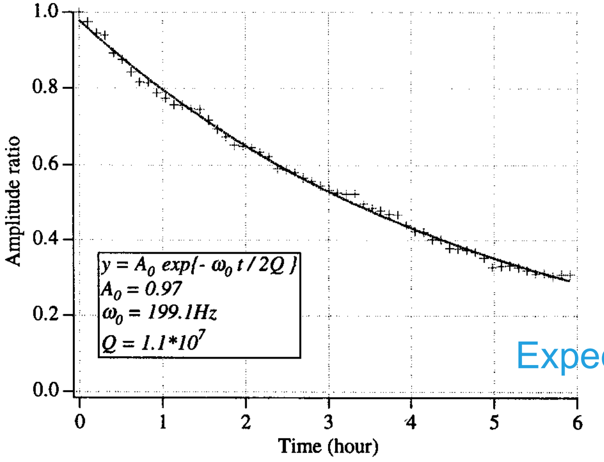

Source: Ushiyama et al., Physics Letters A 273 (2000), DOI: 10.1016/S0375-9601(00)00514-4

Extrinsic losses

- Clamping
- Recoil
- Gas damping
- Eddy currents

Expected values:

$Q_{\text{Sapphire,bulk}} \approx 10^8$

$Q_{\text{Silicon,bulk}} \approx 10^8$

$Q_{\text{Titanium,bulk}} \approx 10^6$

FEM-based sample support system design

Modal analysis of samples

Defines: $f_{\text{natural,sample}}$

Phase 1

- Sapphire and silicon rods with clamped heads
- Empty Ti tubes welded in clamp

Phase 2

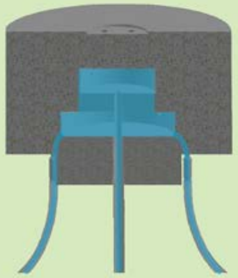

- He-II filled Ti tubes welded in clamp

$f_{\text{natural,sample}}$

Modal analysis of support structure

Defines: $f_{\text{natural,support structure}}$

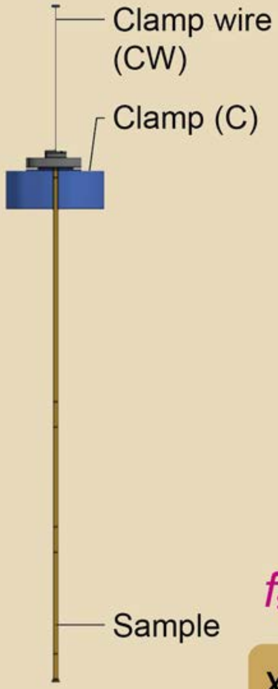

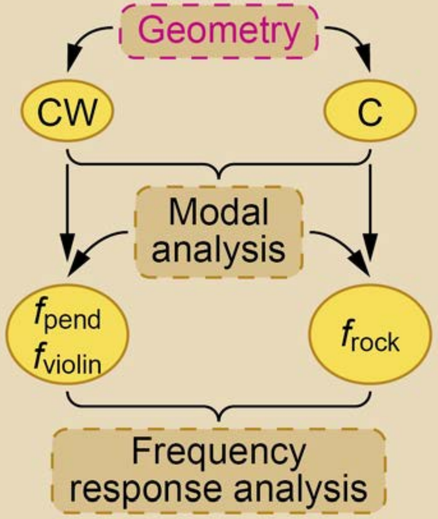

$f_{\text{support structure}} \overset{!}{\neq} f_{\text{sample}}$

$x_{\text{support structure}}$

Energetic evaluation

- Strain energy $\hat{U}_i = U_i / U_{\text{total}}$ yields weighted loss angle estimation
- Determines deployable materials

$$\sum \hat{\phi}_{\text{Set-Up}} = \underbrace{\hat{U}_{SA}\phi_{SA}}_{\hat{\phi}_{\text{intrinsic}}} + \underbrace{\hat{U}_{CW}\phi_{CW} + \hat{U}_{C}\phi_{C}}_{\hat{\phi}_{\text{extrinsic}}}, \quad \hat{\phi}_{\text{intrinsic}} \overset{!}{>} \hat{\phi}_{\text{extrinsic}}$$

Set-up materials	$\phi_{\text{bulk}}(T = 4\text{ K})$
Aluminium	10^{-6}
Ti–6Al–4V	10^{-4}
Tungsten	10^{-6}
SST	10^{-4}
Copper	10^{-4}
Titanium Grade II	10^{-6}

$\hat{\phi}_{\text{Set-up}}$

KIT

Results ➪ Natural frequencies of the samples

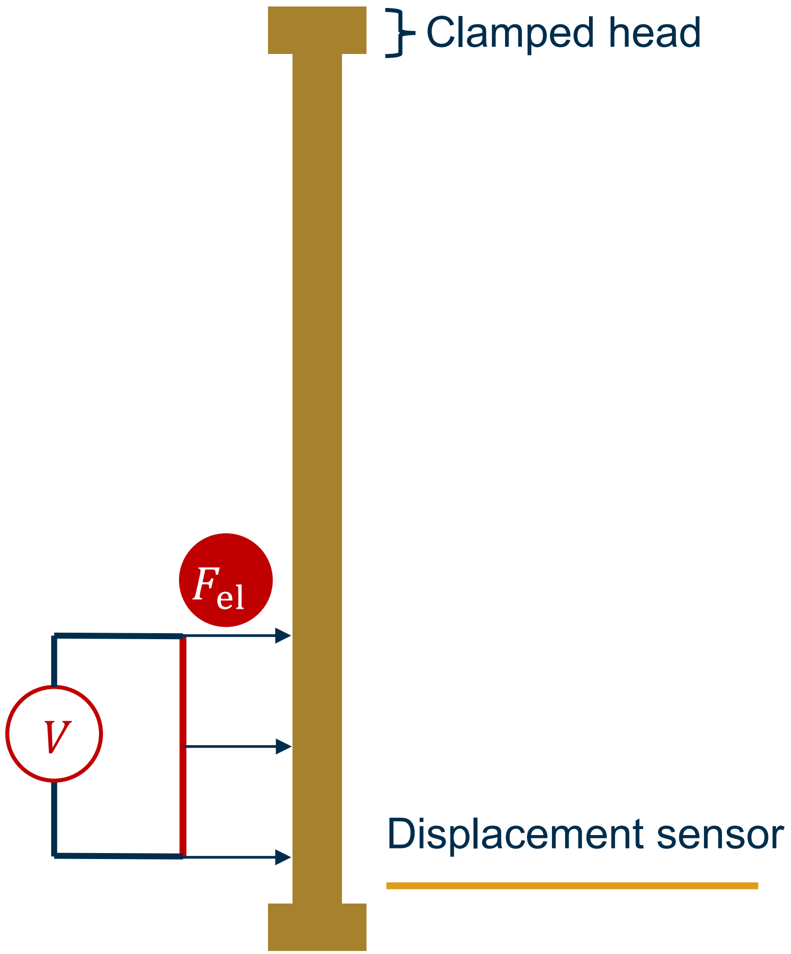

- Modal analyses of samples: $Q = \left(\phi(f_0)\right)^{-1}$

Suspension	$f_{0,1}$/ Hz	$f_{0,2}$/ Hz	$f_{0,3}$/ Hz
Silicon	6	41	120
Sapphire	8	60	205
Titanium tube	5	38	120

Results ➪ Modal analysis of support structure

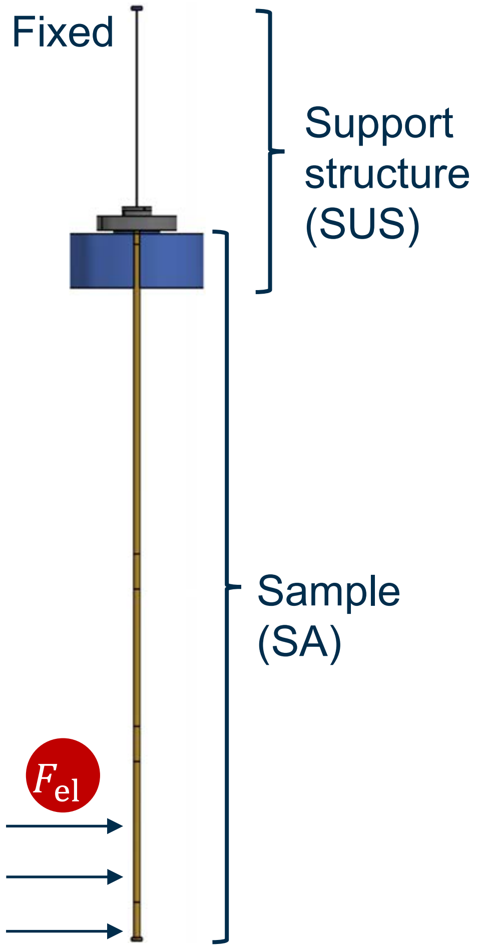

- Modal analysis of support structure: $x_{\text{support structure}}$

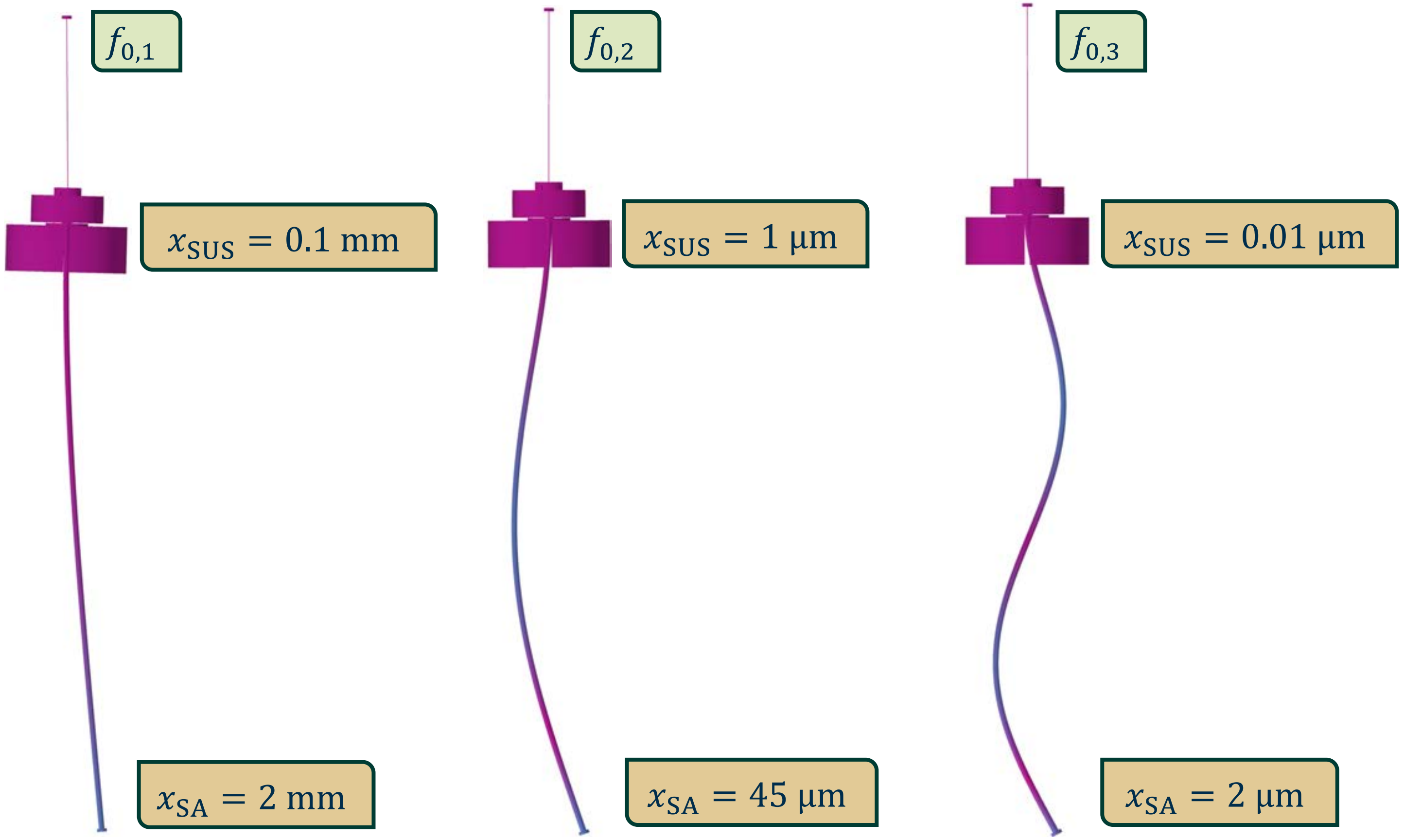

Results ➩ Energetic evaluation

- Loss estimation $\hat{\phi}_{\text{Set-up}}$ of the experimental set-up

Sapphire SA	$\hat{\phi}_{\text{intrinsic}}$	$\hat{\phi}_{\text{extrinsic}}$	$\sum \hat{\phi}_{\text{Set-Up}}$
$f_{\text{SA},1}$	10^{-8}	2×10^{-8}	3×10^{-8}
$f_{\text{SA},2}$	10^{-8}	6×10^{-10}	10^{-8}
$f_{\text{SA},3}$	10^{-8}	3×10^{-10}	10^{-8}

Titanium SA	$\hat{\phi}_{\text{intrinsic}}$	$\hat{\phi}_{\text{extrinsic}}$	$\sum \hat{\phi}_{\text{Set-Up}}$
$f_{\text{SA},1}$	10^{-6}	2×10^{-8}	10^{-6}
$f_{\text{SA},2}$	10^{-6}	2×10^{-8}	10^{-6}
$f_{\text{SA},3}$	10^{-6}	2×10^{-10}	10^{-6}

Design summary

- Titanium grade II upper clamp
- Aluminum lower clamp
- $d_{\text{Clamp}} = 200\text{ mm}$
- $m_{\text{Clamp}} = 10\text{ kg}$
- Ti-6Al-4V clamp suspension
- $d_{\text{clamp suspension}} = 1\text{ mm}$
- $l_{\text{clamp suspension}} = 350\text{ mm}$

Development of the lab-scale He-II supply system

BLUEFORS
CRYOMECH

PT450 Pulse
Tube Cryocooler

- **Design targets**
  - Min. cooling capacity **0.4 W @ 1.8K**
  - Fast cooldown via **warm bypass**
  - Cooling capacity up to **1.0 W @ 1.8K** feasible due to **novel heat exchanger technology**
    - High thermal performance
    - Low pressure loss

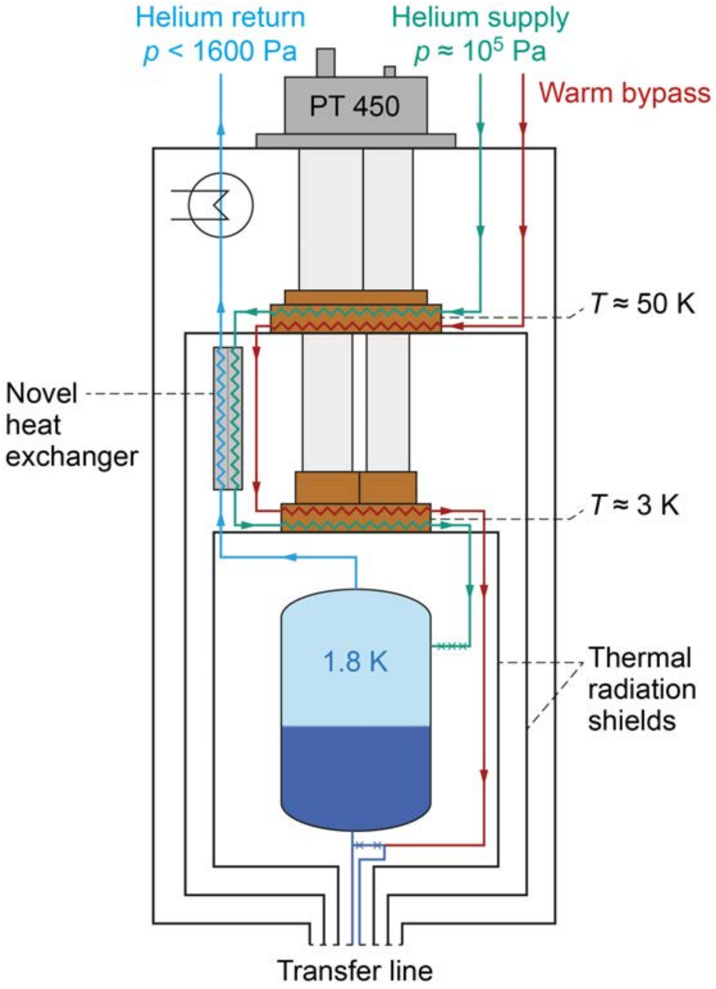

Micro-structured foil-frame counter-flow heat exchanger

Conceptual drawing

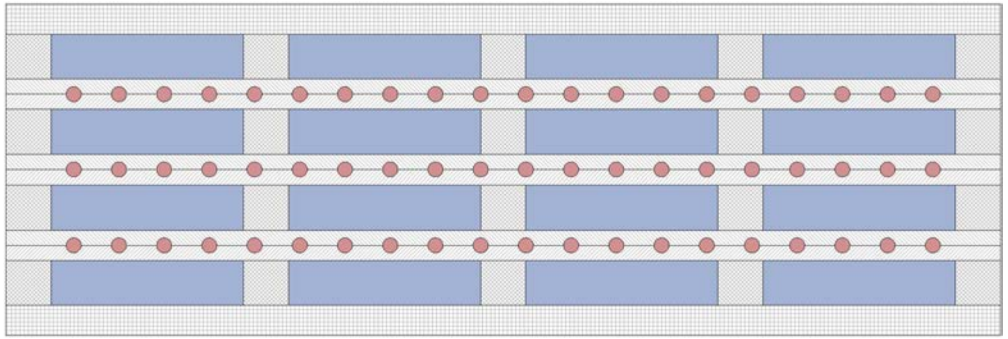

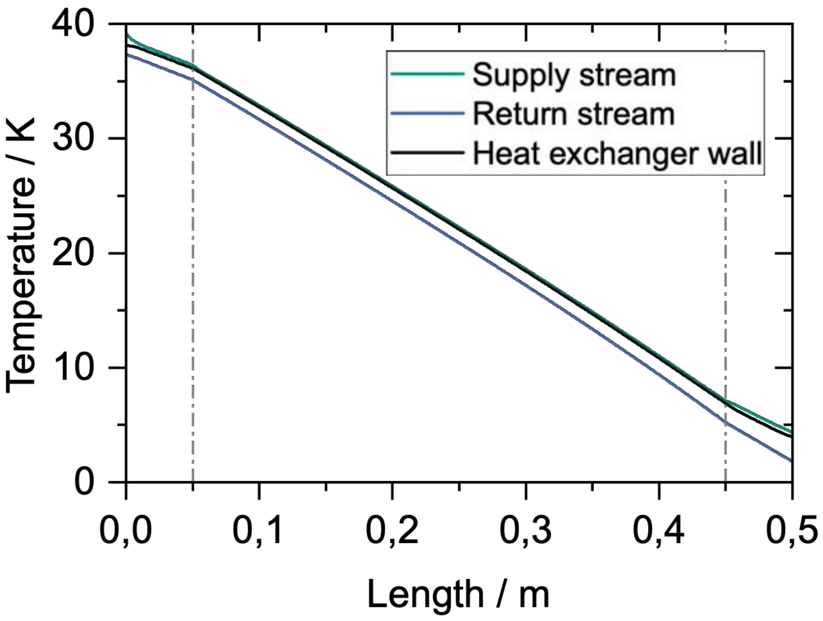

Geometry optimization by Differential Evolution (DE) algorithm

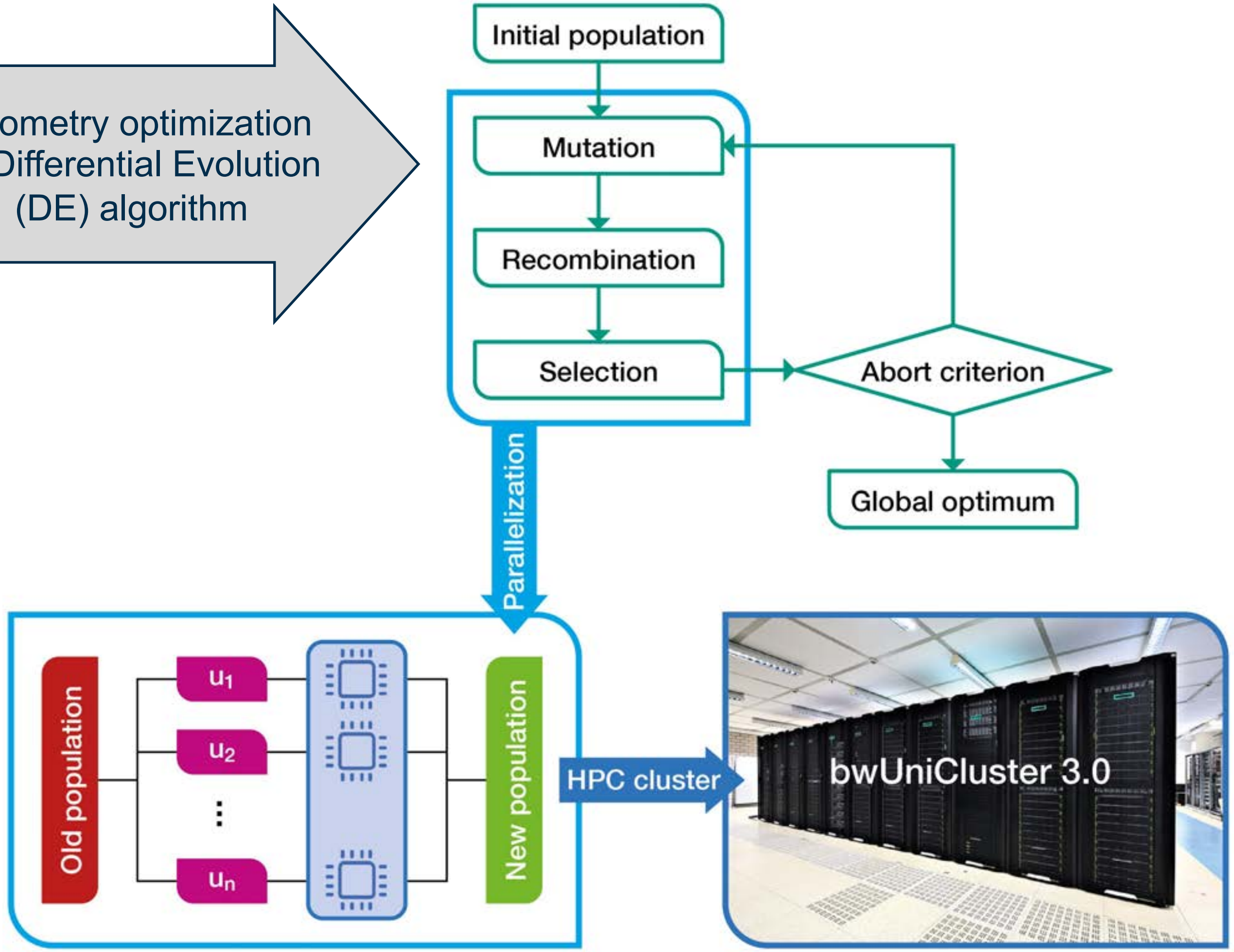

Vibration attenuation system (VAS)

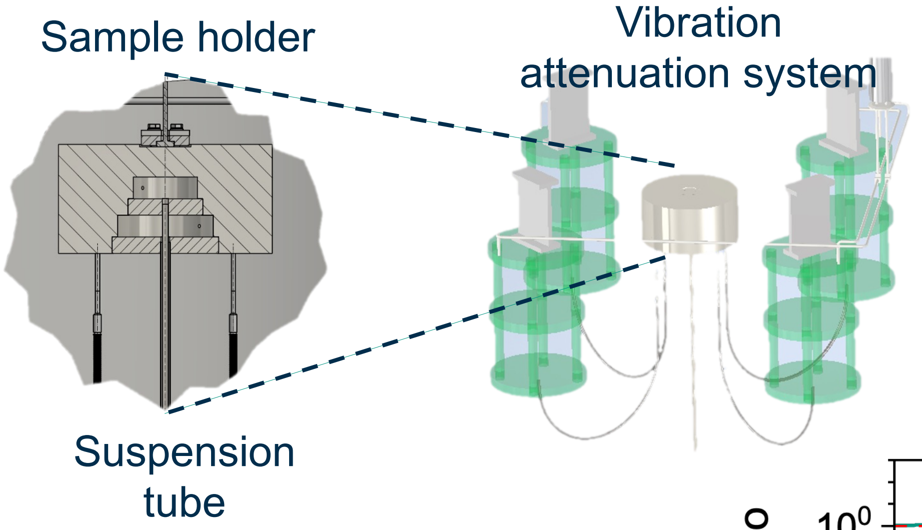

$$\text{Attenuation Ratio} = \frac{\text{Displacement out}}{\text{Displacement in}}$$

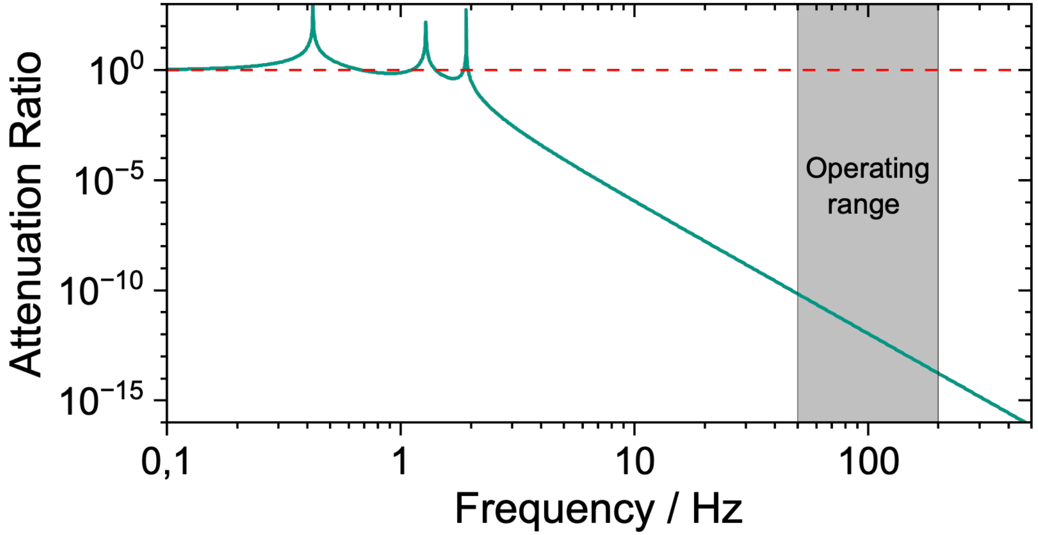

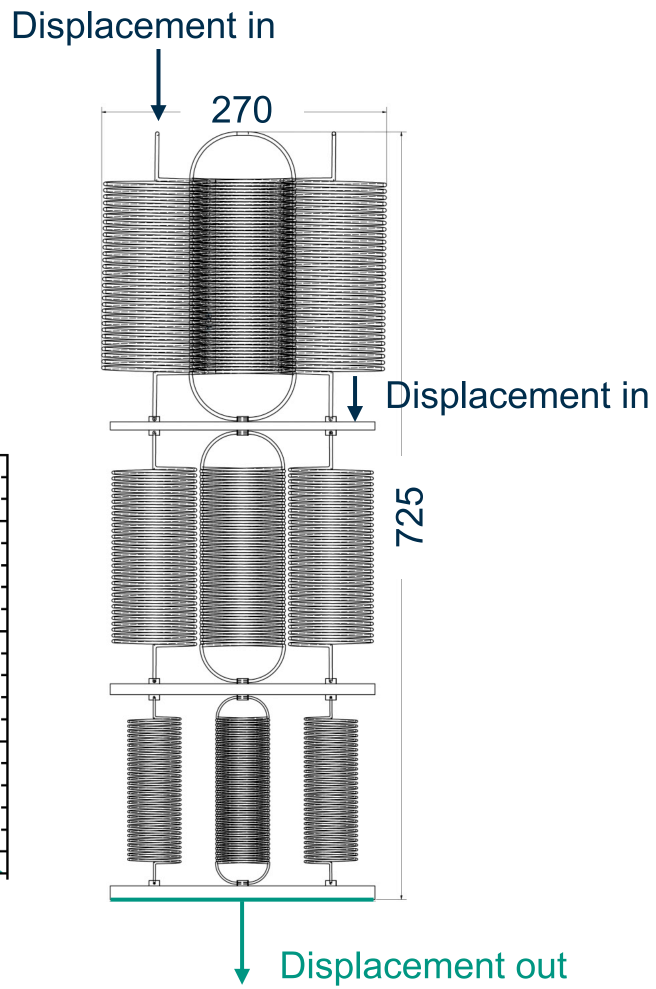

Status and outlook

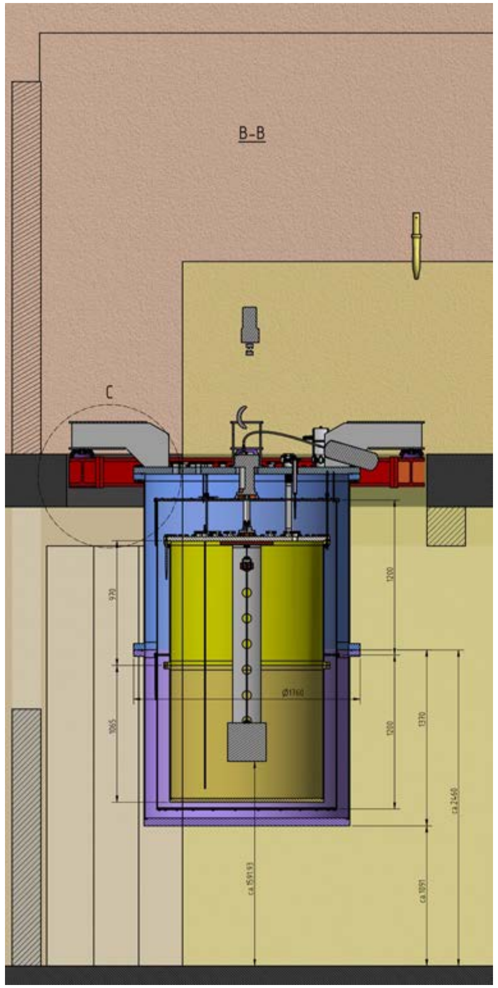

- Main components are ordered (test cryostat, cryocoolers, VAS) ✓
- Installation and commissioning of test cryostat by end 2025 ✓
- Completion of He-II supply system design by end 2025
- Start of Phase 1 experiments beginning 2026

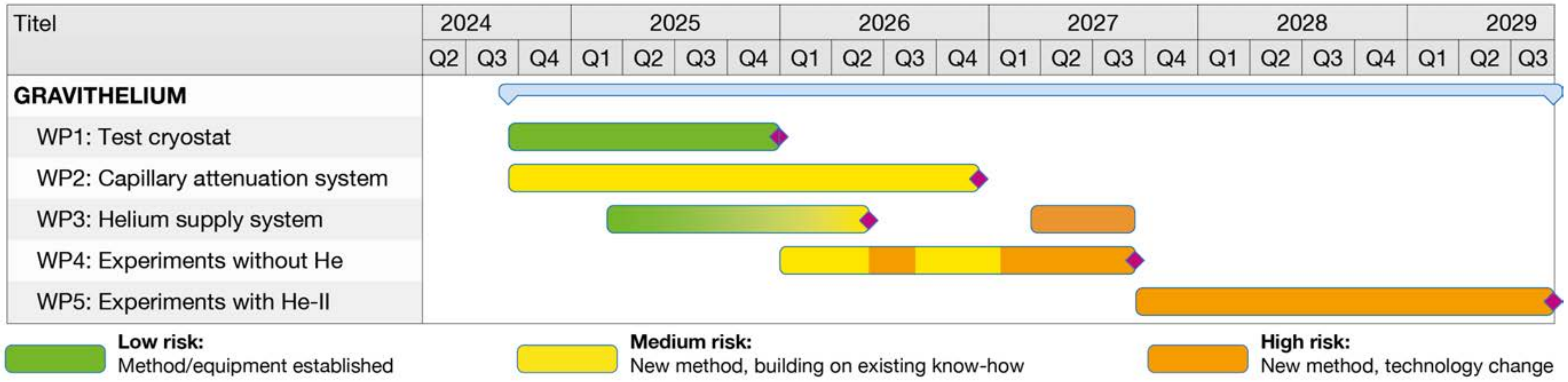

Test cryostat
in experimental hall

Funded by
the European Union

European Research Council
Established by the European Commission

Funded by the European Union (ERC-2023-ADG, GRAVITHELIUM, 101142269). Views and opinions expressed are however those of the author(s) only and do not necessarily reflect those of the European Union or the European Research Council. Neither the European Union nor the granting authority can be held responsible for them.